EXTINCTION CRITERIA FOR OPPOSED-FLOW FLAME SPREAD IN A MICROGRAVITY ENVIRONMENT

SUBRATA BHATTACHARJEE
CHRIS PAOLINI
San Diego State University, San Diego, California

and

KAZUNORI WAKAI
SHUHEI TAKAHASHI
Gifu University, Gifu, Japan

INTRODUCTION: A simplified analysis is presented to extend a previous work [1] on flame extinction in a quiescent microgravity environment to a more likely situation of a mild opposing flow. The energy balance equation, that includes surface re-radiation, is solved to yield a closed form spread rate expression in terms of its thermal limit, and a radiation number that can be evaluated from the known parameters of the problem. Based on this spread rate expression, extinction criterions for a flame over solid fuels, both thin and thick, have been developed that are qualitatively verified with experiments conducted at the MGLAB [2] in Japan. Flammability maps with oxygen level, opposing flow velocity and fuel thickness as independent variables are extracted from the theory that explains the well-established trends in the existing experimental data [3].

Thermal Regime: An energy balance for the solid phase control volume of Fig. 1 can be written as.

$$\lambda_g \frac{\left(T_f - T_v\right)}{L_g} L_g - \varepsilon\sigma\left(T_v^4 - T_\infty^4\right) L_g \sim V_f \rho_s c_s \tau_h \left(T_v - T_\infty\right) \tag{1}$$

where, T_f and T_v are characteristic flame and vaporization temperature, τ_h is the thickness of the heated layer, and $L_g = \alpha_g / \left(V_f + V_g\right)$ is the gas-phase length scale. For thin fuels in the thermal limit, $\tau_h = \tau$ and $\varepsilon = 0$ produces the de Ris solution $V_{f,\text{th,thn}} \sim \left(\lambda_g / \rho_s c_s \tau\right) F$, where $F \equiv \left(T_f - T_v\right)/\left(T_v - T_\infty\right)$. Using $V_{f,\text{th,thn}}$ to non-dimensionalize V_f , $\eta_f \equiv V_f / V_{f,\text{th,thn}}$ Eq. (1) can be expressed in non-dimensional form as follows.

$$\left(\eta_f^2 + \eta_f \eta_g\right)\frac{\tau_h}{\tau} - \left(\eta_f + \eta_g\right) + \Re_0 \sim 0 \text{; where, } \Re_0 \equiv \frac{1}{F^2}\frac{\rho_s c_s}{\rho_g c_g}\frac{\varepsilon\sigma\tau}{\lambda_g}\left(\frac{T_v^4 - T_\infty^4}{T_v - T_\infty}\right),\ \eta_g \equiv \frac{V_g}{V_{f,\text{th,thn}}} \tag{2}$$

The thermal thin limit $\eta_{f,\text{th,thin}} \sim 1$ is recovered when $\Re_0 = 0$ and $\tau_h = \tau$. To obtain a more general solution τ_h / τ for a thick fuel can be scaled as

$$\frac{\tau_h}{\tau} \sim \frac{\sqrt{\alpha_s t_{\text{res,s}}}}{\tau} \sim \sqrt{\frac{\alpha_s L_g}{\tau^2 V_f}} \sim \frac{\Omega}{F}\frac{1}{\sqrt{\eta_f\left(\eta_f + \eta_g\right)}} \quad \text{where, } \Omega \equiv \sqrt{\frac{\lambda_s \rho_s c_s}{\lambda_g \rho_g c_g}} \ . \tag{3}$$

Substituting this into Eq. (2) and still ignoring radiation, we obtain the thermal limit for semi-infinite fuel beds.

$$\eta_{f,\text{th,thick}} \sim \frac{F^2}{\Omega^2}\eta_g\left(1 - \frac{F^2}{\Omega^2}\right)^{-1} \sim \frac{F^2}{\Omega^2}\eta_g \quad \text{if } \tau \ge \tau_h;\ \text{or, } \tau \ge \frac{\lambda_s}{\rho_g c_g V_g F};\ \text{ or, } \ \eta_g \ge \frac{\Omega^2}{F^2} \tag{4}$$

The simplification above is achieved because for both PMMA and cellulose it can be shown that $F < \Omega$. Equation (4) also provides a criterion for transition between the thin and the thick limit for $\eta_g \gg 1$. Prediction from Eq. (4)

is plotted in Fig. 2 showing the transition from the thin to the thick limit in the thermal regime. Not much data in the thick-thin transitional region is available to verify this simple transition criterion.

Radiative Regime: The energy balance equation, Eq. (2), is solved in both the thick and thin limit producing

Thin Limit: $\eta_{f,\text{thin}} \sim \dfrac{1-\eta_g}{2} + \dfrac{1}{2}\sqrt{\left(1+\eta_g\right)^2 - 4\Re_0}$; **Thick Limit:** $\eta_{f,\text{thick}} \sim \dfrac{F^2}{\Omega^2}\eta_g\left(1-\dfrac{\Re_0}{\eta_g}\right)^2$; (5)

These results are plotted in Figs. 3 and 4 for several values of the radiation parameter $\Re_0$. A number of important features of the radiative effects on flame spread rates are revealed by these plots. When $\Re_0 > 0$, the slope of the spread rate curves decreases with opposing velocity for thin fuels while this trend is completely reversed for thick fuels. The MGLAB data [2] for flame spread over thin PMMA, shown in Fig 5, support this predicted trend for thin fuels. The DARTFIRE experiments [4] for flame spread over thick PMMA lends supports to the trends predicted by Fig. 4.

Obvioulsy, for $\Re_0 = 0$ and/or $\eta_g \to \infty$, the thermal limits are recovered with $\eta_{f,\text{thin}} = 1$ and $\eta_{f,\text{thick}}$ being proportional to η_g. To establish a criterion for the transition between the thermal and radiative regimes, we simplify Eq. (5) assuming $\eta_g \gg 1$. If the spread rate is non-dimensionalized by the corresponding thermal limit, Eq. **Error! Reference source not found.** for both the thick and thin limit can be shown to approach the same form.

Thin and Thick Fuels: For $\eta_g \gg 1$, $\eta'_f \equiv \dfrac{V_f}{V_{f,\text{thermal}}} \sim \left(1-\dfrac{\Re_0}{\eta_g}\right)^2 \sim 1-2\Re_V$; where, $\Re_V \equiv \dfrac{\Re_0}{\eta_g}$ (6)

A single parameter $\Re_V$, therefore, controls the radiative effects on the spread rate for both thermally thin and thick fuels. η'_f from Eq. (6) is plotted in Fig. 6 against versus $1/\Re_V$, so that the abscissa is proportional to V_g. Superposed on this figure are experimental spread rates from MGLAB experiments, only part of which were previously reported [2]. Although the spread of the data around the prediction of Eq. (6) is substantial, the onset of radiative effects seems to be well correlated by the analytical prediction.

Extinction Criteria: The spread rate expressions of Eq. (5) can be used to establish criterion for flame extinguishment. As can be seen from Figs. 3 and 4, there are two types of extinction behavior. For $\eta_g \geq 1$, in both the thin and thick limit, steady flame cannot be sustained provided $\eta_g > \Re_0$, a criterion that is independent of fuel thickness. For $\eta_g < 1$, the thick fuel criterion remains unaltered. However for thin fuels, the spread rate assumes complex values, an indication of extinguishment, when $\eta_g < 2\sqrt{\Re_0}\text{-}1$. For flame spread over PMMA, these criteria are combined in the flammability map of Fig. 7. Note that for a critical thickness can be calculated from the relation $\eta_g = \Re_0 = 1$, beyond which extinction is independent of fuel thickness, thereby, defining a radiatively thick fuel.

Conclusion

In this article we present a simplified analysis to develop for the first time a closed-form expression for the spread rate and extinction criterion for flame spread over condensed fuels in a mild opposing-flow microgravity environment. The results presented are supported by experiments on thin PMMA conducted in the MGLAB.

Acknowledgement: Support from NASA, Glenn Research Center, with Dr. Sandra Olson as the contract monitor, is gratefully acknowledged.

REFERENCES: [1] Bhattacharjee, S., Takahashi, Wakai, K., A., *Prediction of a Critical Fuel Thickness for Flame Extinction in a Quiescent Microgravity Environment,* Combustion and Flame, to appear, 2003

[2] Takahashi, S., Kondou, M., Wakai, K., A., Bhattacharjee, S., Proceedings of the Combustion Institute, Vol 29, 2002.)

[3] Olson, S.L., Ferkul, P.V., and T'ien, J.S., Proceedings of the Combustion Institute, 22:1213, (1988)

[4] Altenkirch, R.A, Olson, S., and, Bhattacharjee, S., "Diffusive and Radiative Transport in Fires", NASA Contract NCC3-221 (1993-1998)

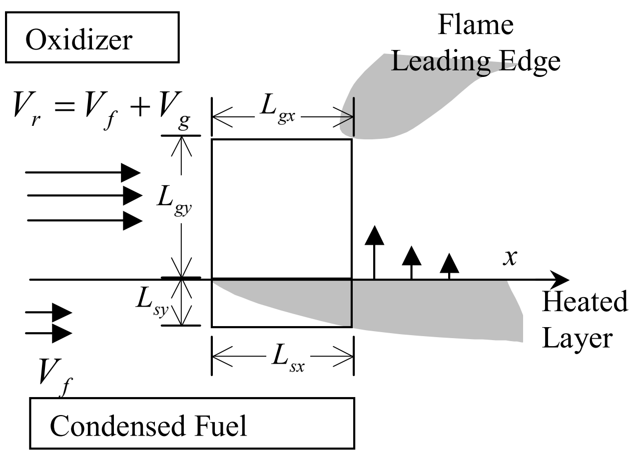

Fig. 1 Control volumes at the flame leading edge in the gas and the solid phases.

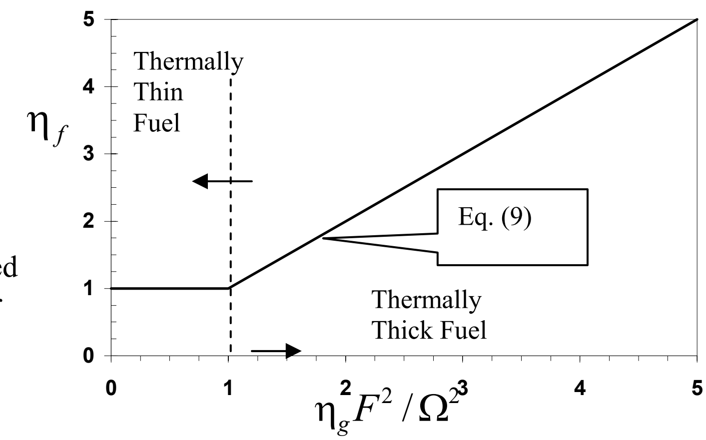

Fig. 2. Non-dimensional spread rate in the thermal regime.

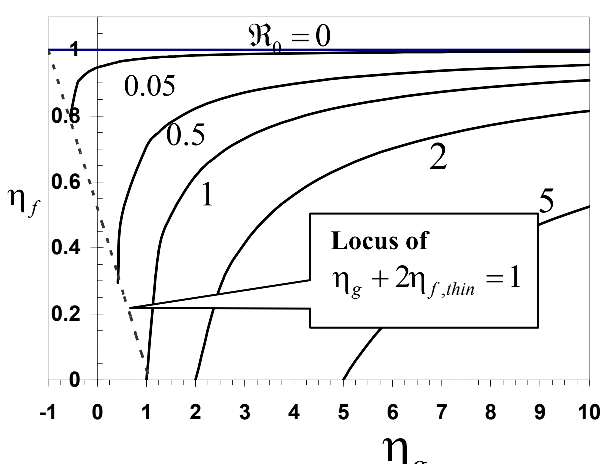

Fig. 3. Spread rate as a function of η_g and $\Re_0$ as predicted by Eq. (7). Opposed-flow flame spread extends down to $\eta_g = -1$.

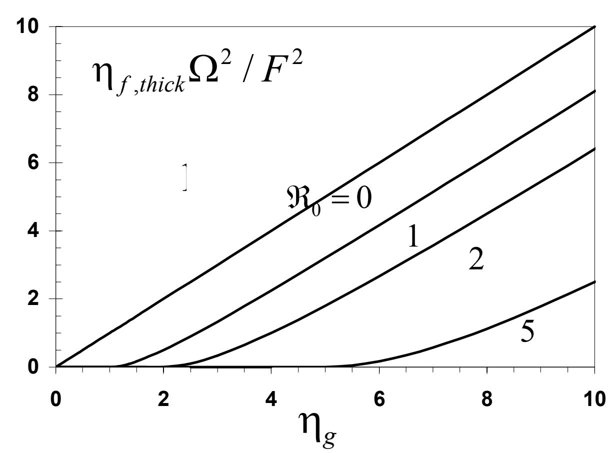

Fig. 4. Spread rate for thick fuel as a function of η_g and $\Re_0$ as predicted by Eq. (7). The spread rate is zero (extinction) for $\eta_g < \Re_0$.

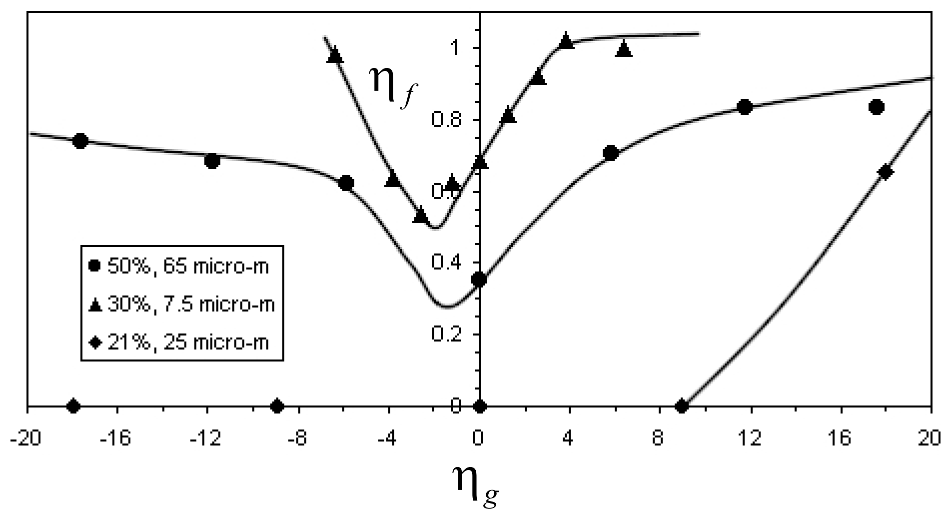

Fig. 5. Non-dimensional experimental spread rate [9] as a function of η_g for different oxygen mole fractions and fuel half-thickness. Note that in this plot the highest experimental spread rate is used to normalize V_f and V_g instead of the theoretical thermal limit.

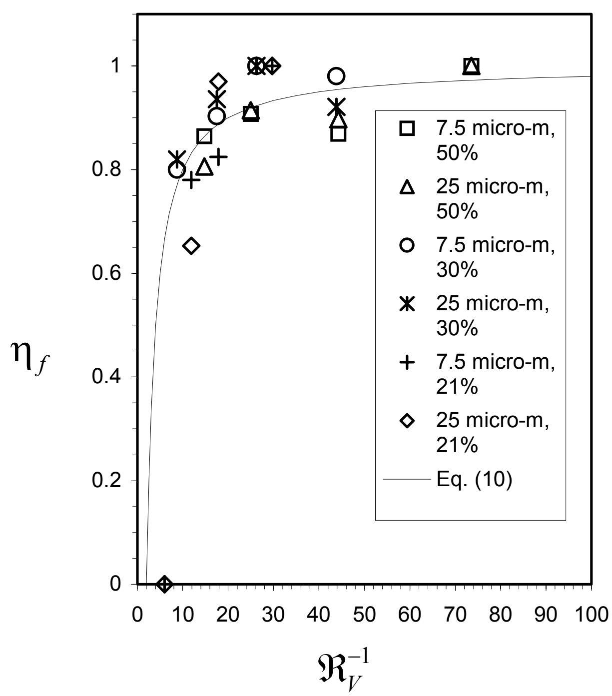

Fig. 6. Prediction of the non-dimensional spread rate η_f plotted as a function of inverse of $\Re_{0,thin}$ from Eq. (10). The prediction is compared with the spread rate data from the MGLAB experiments.

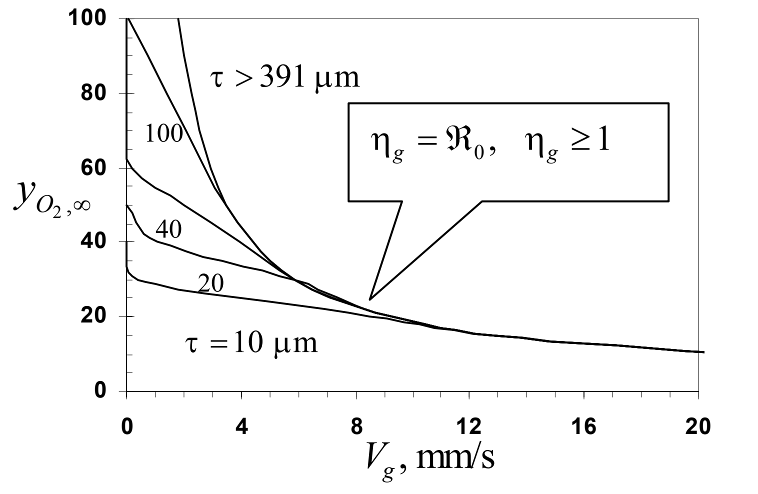

Fig. 7. Flammability map for PMMA fuel at various half-thickness at 1 atm. Radiative extinction happens on the left side of each curve.